

# Magnitude and Molecular Origin of Water Slowdown Next to a Protein

Fabio Sterpone,<sup>\*,‡</sup> Guillaume Stirnemann,<sup>¶</sup> and Damien Laage<sup>\*</sup>

Department of Chemistry, Ecole Normale Supérieure, UMR ENS-CNRS-UPMC 8640, 24 rue Lhomond, 75005 Paris, France

**S** Supporting Information

**ABSTRACT:** Hydration shell dynamics plays a critical role in protein folding and biochemical activity and has thus been actively studied through a broad range of techniques. While all observations concur with a slowdown of water dynamics relative to the bulk, the magnitude and molecular origin of this retardation remain unclear. Via numerical simulations and theoretical modeling, we establish a molecular description of protein hydration dynamics and identify the key protein features that govern it. Through detailed microscopic mapping of the water reorientation and hydrogen-bond (HB) dynamics around lysozyme, we first determine that 80% of the hydration layer waters experience a moderate slowdown factor of  $\sim 2$ – $3$ , while the slower residual population is distributed along a power-law tail, in quantitative agreement with recent NMR results. We then establish that the water reorientation mechanism at the protein interface is dominated by large angular jumps similar to the bulk situation. A theoretical extended jump model is shown to provide the first rigorous determination of the two key contributions to the observed slowdown: a topological excluded-volume factor resulting from the local protein geometry, which governs the dynamics of the fastest 80% of the waters, and a free energetic factor arising from the water–protein HB strength, which is especially important for the remaining waters in confined sites at the protein interface. These simple local factors are shown to provide a nearly quantitative description of the hydration shell dynamics.

The water layer surrounding a protein is considered to be an indispensable lubricant that facilitates conformational rearrangements occurring, e.g., during folding,<sup>1</sup> molecular recognition, and enzyme catalysis.<sup>2</sup> The peculiar dynamical properties of the hydration layer have thus been extensively studied through a broad range of experimental<sup>2d,3</sup> and computational<sup>3k,l,4</sup> techniques. All of these techniques have observed that hydration waters are slowed compared to the bulk, but the measured retardation factors range from a moderate 2-fold<sup>3c</sup> up to dramatic slowdowns by several orders of magnitude.<sup>3e</sup> This has led to great confusion about the behavior of water in biochemical environments, and a detailed understanding of protein hydration dynamics has remained elusive. Essential aspects are still unclear, including the exact magnitude of the slowdown induced by a protein interface, but also the specific protein features and mechanisms that

determine this slowdown (e.g., its shape or the chemical nature of its exposed groups) and whether water motions within the hydration layer are significantly more collective than in the bulk.<sup>4c,d</sup>

Here, we address these key outstanding questions by combining molecular dynamics simulations with a recently proposed<sup>5</sup> analytic jump reorientation model for water, in order to determine the origin and magnitude of this slowdown. The reorientation dynamics is shown to be essentially determined by an activated jump between hydrogen-bond (HB) acceptors, and the model clearly establishes the different protein contributions to the jump activation free energy barrier. Instead of adding yet another measurement of protein hydration dynamics with a new technique, this model provides an understanding of the physical mechanisms that govern the slowdown induced by the protein interface and rigorously identifies the relevant protein features.

We selected lysozyme as our paradigm system, a globular protein whose hydration dynamics has already been extensively investigated through both experiments<sup>3b,f,1</sup> and simulations.<sup>4g,6</sup> Our analysis is based on a molecular dynamics trajectory of a fully hydrated lysozyme simulated at ambient conditions, in a neutral pH protonation state.<sup>7</sup>

We first characterized the reorientation dynamics of water at the protein interface. The average orientational relaxation of waters initially in the protein hydration shell exhibits a much slower decay than in the bulk (Figure 1a). Its pronounced nonexponential character reveals the presence of a strong dynamical heterogeneity within the hydration shell, caused by a broad distribution of reorientation times. By calculating the reorientation next to each protein site separately, we explicitly determined this distribution, which is broad and asymmetric (Figure 1b). Most first-shell water molecules experience a limited slowdown relative to the bulk, with an average 2.3 slowdown factor for the fastest 90% of the water molecules, in excellent agreement with the value of 2 recently determined by NMR for a set of similar globular proteins.<sup>3c</sup> Our simulations further indicate that the fraction of first-shell waters experiencing a slowdown  $>10$  is completely negligible ( $<1\%$ ), and these essentially correspond to deeply buried structural waters.

The computed distribution can be approximated as the sum of a tall, narrow Gaussian centered on moderate slowdowns together with a power-law tail  $1/\tau^\alpha$ , with  $\alpha = 2.4 \pm 0.5$  for greater slowdowns. This exponent is again consistent with both

Received: January 24, 2012

Published: February 15, 2012

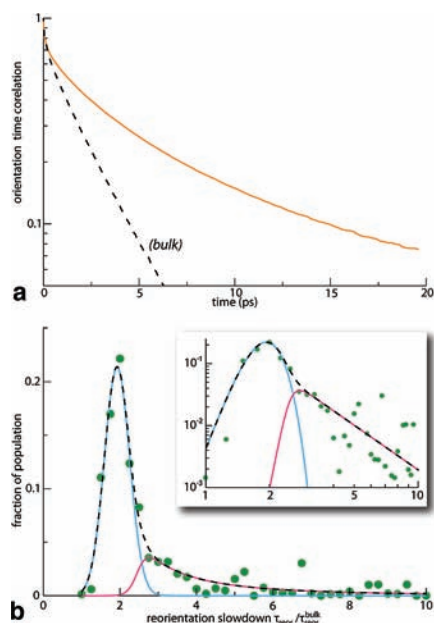


**Figure 1.** (a) Orientation time correlations averaged over all the water molecules initially within the protein hydration layer and within the bulk. (b) Probability distribution of the water reorientation slowdown relative to the bulk within lysozyme's first hydration shell (green dots), together with a fit combining a Gaussian distribution (blue) and a power-law tail (pink). The inset shows the same data on a log–log scale. The bulk reference reorientation time is  $\tau_{\text{reor}}^{\text{bulk}} = 2.5$  ps. The mean reorientation slowdown within the entire hydration shell is 3.8.

prior NMR studies on globular proteins (BPTI, ubiquitin, and  $\beta$ -lactoglobulin), which postulated a power-law distribution and obtained values of 2.1–2.3,<sup>3c</sup> and other simulation studies, which showed that the water residence time at the protein interface is distributed along a power-law, with similar values of the exponent for similar proteins ( $\alpha = 2.5$  for cytochrome *c*<sup>8a</sup> and  $\alpha = 1.7$  for plastocyanin<sup>8b</sup>) and a smaller value for a larger protein ( $\alpha = 0.8$  for acetylcholinesterase<sup>8c</sup>). As previously anticipated,<sup>3c</sup> we also note that, while the commonly used stretched-exponential fit may be satisfactory for the average orientational time correlation decay,<sup>4c,d,g</sup> its associated distribution of reorientation times markedly differs from our computed distribution, which casts doubt upon the validity of arguments assigning the nonexponential behavior to a collective glassy behavior within the hydration shell.<sup>4c,d</sup>

To understand the origin of the spread in hydration dynamics and predict how it changes, e.g., with the protein sequence and conformation, we first computed the spatial distribution of the water slowdowns on the protein exposed surface. Such site-resolved mapping is a long-standing goal of experimental protein hydration studies, but despite recent breakthroughs it remains only accessible through simulations since all experimental techniques to date require strongly perturbing the system, e.g., through mutations<sup>3c</sup> or confinement.<sup>9</sup> Figure 2 shows that, while the protein interface is very rough and chemically heterogeneous, the slowdown relative to the bulk is strikingly similar and moderate ( $\sim 2$ -fold) throughout the hydration shell. The slowest water molecules are located within the inner part of the active-site cleft (blue patch in Figure 2b). Outside the active-site cleft, no clear clustering of sites with similar hydration dynamics can be seen, in contrast with recent experiments performed on a protein confined within a reverse micelle.<sup>9</sup> This difference is most

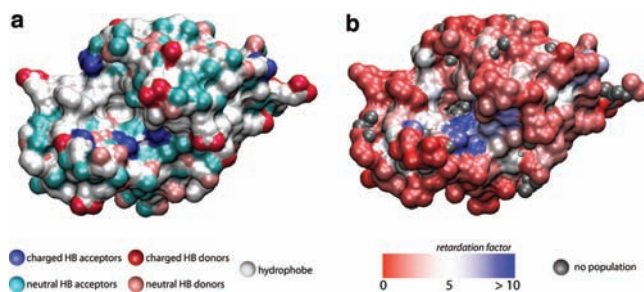


**Figure 2.** (a) Mapping on the lysozyme surface of the chemical nature of the exposed groups, showing the alternation of hydrophobic, charged, and polar HB donor and acceptor groups. (b) Mapping of the water reorientation slowdown relative to the bulk; the very slow region lies within the active-site cleft. No or very little water population was found next to the gray sites.

probably another manifestation of the strong perturbation of the protein induced by the interaction with the reverse micelle, as recently detailed in a simulation study.<sup>10</sup> The quite uniform retardation observed in our mapping may explain why prior attempts<sup>4b,11</sup> fell short of finding a clear connection between hydration dynamics and the protein topology or the types of exposed groups. However, we now show that this missing link can be provided by the molecular jump picture,<sup>5a</sup> which has already successfully described water reorientation next to a wide range of solutes.<sup>5b,12</sup>

This novel picture originated from the observation that bulk water mainly reorients through sudden large-amplitude angular jumps when a water hydroxyl (OH) group trades HB acceptors.<sup>5,13</sup> The contribution of these angular jumps to the reorientation time is determined by the jump amplitude  $\Delta\theta$  and the jump time  $\tau_{\text{jump}}$  separating successive jumps.<sup>5</sup> An additional, usually minor contribution  $\tau_{\text{reor}}^{\text{frame}}$  comes from the slower tumbling of the molecular frame for an OH involved in an intact HB between HB acceptor exchanges.<sup>5</sup> In bulk water at 300 K, the (second-order) reorientation times arising from these two contributions are respectively 3.6 and 5.6 ps. The extended jump model (EJM) combines these two independent reorientation pathways to yield the overall EJM reorientation time.<sup>5,7</sup>

For each protein site, the three ingredients of the EJM ( $\tau_{\text{jump}}$ ,  $\Delta\theta$ , and  $\tau_{\text{reor}}^{\text{frame}}$ ) were determined for all water molecules in its hydration layer, and the global distribution of the EJM reorientation times was reconstructed.<sup>7</sup> Figure 3a shows that the EJM remarkably reproduces all the key features of the directly computed distribution, including the peak at moderate slowdown values and the long tail. As shown in Figure 3b, for  $>80\%$  of the water molecules, the EJM prediction is within 20% of the directly computed slowdown. (Factors causing the small residual differences between the EJM and the direct calculation are detailed in ref 7.) This clearly shows that, despite the complexity of the protein environment, the jump picture developed for water in the bulk<sup>5</sup> and next to simpler solutes,<sup>5b</sup> including ions,<sup>14</sup> amphiphilic molecules<sup>12a</sup> (e.g., osmolytes), and dilute amino acids,<sup>12b</sup> remains an adequate description of the water reorientation mechanism.

Figure 3a also shows that the reorientation and HB jump slowdown distributions are similar, evidence that large angular jumps due to HB acceptor exchanges remain the dominant reorientation pathway for hydration shell waters (except for 7% of the shell next to very strong HB acceptor sites, e.g., aspartate and glutamate carboxylate groups, as already found for dilute

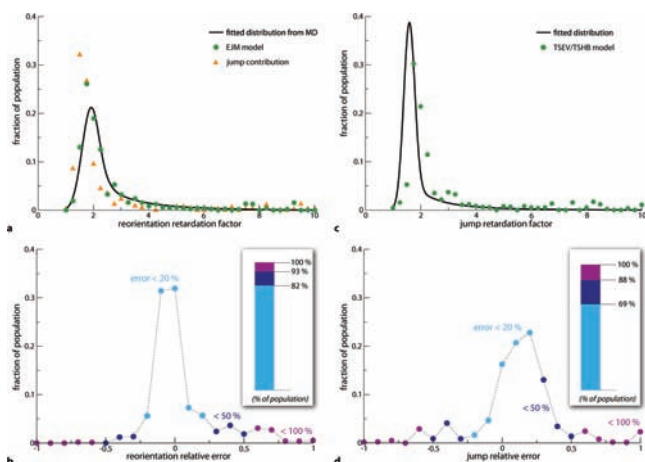


**Figure 3.** (a) Probability distribution of the reorientation slowdown factor  $\rho = \tau_{\text{reor}}/\tau_{\text{reor}}^{\text{bulk}}$  computed via the EJM (green) compared with the fit of the directly computed distribution (black, see Figure 1) for waters within the lysozyme hydration shell, together with the distribution of slowdown factors for the jump times  $\tau_{\text{jump}}/\tau_{\text{jump}}^{\text{bulk}}$  (orange). The small shift between the EJM and jump distributions originates from the reduced importance of the frame contribution next to the protein relative to the bulk. (b) Distribution of relative errors between the EJM and directly computed reorientation slowdowns. (c) Probability distribution of the jump slowdown factor  $\rho = \tau_{\text{jump}}/\tau_{\text{jump}}^{\text{bulk}}$  computed via the TSEV/TSHB model (green) compared with the fit of the directly computed distribution (black). (d) Distribution of relative errors between the TSEV/TSHB prediction and the directly computed jump slowdown.

amino acids<sup>12b</sup>). The distribution of reorientation times can thus be understood by analyzing the distribution of jump times between HB acceptors. This is extremely valuable since a jump between HB acceptors can be fruitfully viewed as a chemical reaction in which HBs are broken and formed concertedly,<sup>5</sup> and whose rate constant proceeds from an activation free energy. At the interface between a solute and the bulk, this reaction barrier and the resulting jump kinetics were recently shown to depend on two key local solute features.<sup>5b</sup>

The first effect is topological and is induced by any type of solute and interface.<sup>5b,12a</sup> It results from the partial hindrance of a new water HB partner approach. Compared to the bulk situation, the volume occupied by the solute reduces the number of accessible transition-state (TS) configurations for the jump exchange and leads to a transition-state excluded volume (TSEV) slowdown  $\rho_V$  in the jump rate.<sup>7,12a</sup> The second factor results from the strength of the initial HB that must be elongated to reach the TS configuration. Compared to the bulk situation, this transition-state hydrogen-bond (TSHB) strength factor  $\rho_{\text{HB}}$  accelerates the jump rate if the initial bond is weaker than a water–water HB, and slows the rate if the bond is stronger.<sup>7,12b</sup>

The overall slowdown factor results from the combination of the TSEV and TSHB factors,<sup>5b,12b</sup>  $\rho = \tau_{\text{jump}}^{\text{interface}}/\tau_{\text{jump}}^{\text{bulk}} = \rho_V \times \rho_{\text{HB}}$ , which clearly separates the respective contributions from the protein topology, i.e., the secondary and tertiary structures with the resulting locally concave or convex character of the exposed protein surface ( $\rho_V$ ), and from the interaction free energy between water and the exposed acceptor groups, i.e., from the chemical nature of the protein exposed groups ( $\rho_{\text{HB}}$ ). This analysis presents two major improvements over previous computational approaches: (i) it does not require perturbing the system, e.g., by making the protein apolar,<sup>4a</sup> and (ii) the

relevant local factors are directly identified through the understanding of the water reorientation mechanism, not by a heuristic approach testing different protein features to find which one is best correlated with the water dynamics.<sup>11</sup> Figure 3c shows that, despite their simplicity, the  $\rho_V$  and  $\rho_{\text{HB}}$  factors provide a good prediction of the HB jump time, and the molecular origin of the slowdown factors can now be elucidated by determining the  $\rho_V$  and  $\rho_{\text{HB}}$  components of the overall slowdown factor induced by each protein site (Figure 4).

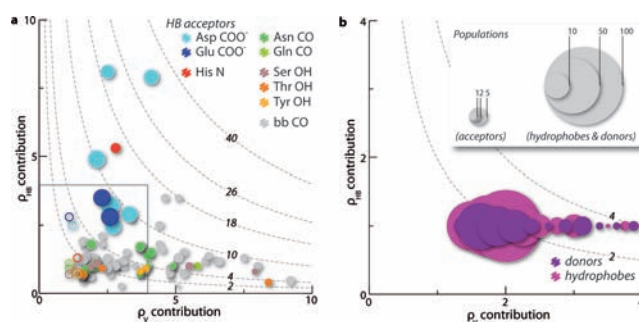


**Figure 4.** Contour plots of the overall retardation factor  $\rho$  along its two components  $\rho_V$  and  $\rho_{\text{HB}}$  for water next to side chain and backbone (bb) sites. Each disk or square corresponds to a type of protein site: its color depends on the site chemical nature and its size scales with the number of affected waters (the scales are shown in the inset and differ for the two panels). The dashed contour lines show the  $\rho$  value. The HB acceptor sites are shown in (a), with the dilute amino acid values indicated by open circles,<sup>12b</sup> and the hydrophobic and HB donor sites are shown in (b). Panel (b) focuses on the area within the gray box in (a).

For 80% of the hydration layer waters, the dynamics is <3 times slower than in the bulk (Figure 1), and comparing the populations with  $\rho < 3$  in Figure 4 unambiguously shows that these waters mostly lie next to hydrophobic and HB donor groups. This slowdown is thus due to an excluded volume effect, i.e., to the local curvature of the protein surface. This important point explains, e.g., why NMR studies<sup>3c</sup> observed the same dynamical behavior within the hydration layer of several globular proteins (and also of small solutes with extended hydrophobic groups): for all these solutes, the hydration dynamics is dominated by the same excluded volume effects.

The remaining, more retarded 20% of the hydration layer present in the distribution's tail corresponds to sites confined within superficial pockets and clefts, where the excluded volume is high,  $\rho_V > 2$  (Figure 4). Most of these sites are HB acceptor groups.<sup>7</sup> For intermediate slowdown factors ( $3 < \rho < 6$ ), the dominant effect is the excluded volume, while for the most retarded sites ( $\rho > 6$ ), the slowdown factor is essentially controlled by the HB strength factor  $\rho_{\text{HB}}$ .<sup>7</sup>

From our results, HB acceptors appear to have a greater influence on water dynamics than HB donors, even when their interaction strengths with water are similar. Since water reorients about an axis that approximately runs through its oxygen, the same force leads to a greater torque when applied by an HB acceptor on the water hydrogen than when applied by an HB donor on the water oxygen.<sup>7</sup> This effect is further reinforced by our choice to follow water dynamics through the OH bond reorientation, motivated by the importance of HB exchanges in water reorientation. Monitoring water reorientation through another vector, such as that normal to the water plane,<sup>3c</sup> could reduce the apparent slowdown factor induced by

HB acceptor sites and increase the relative weight of the moderately retarded peak compared to the slower tail in the distribution.

The success of the  $\rho_V$  and  $\rho_{HB}$  local factors in describing the overall slowdown strongly suggests that protein hydration dynamics can be understood through a simple local approach. Invoking more collective arguments, e.g., a glass-like behavior of the hydration layer,<sup>4c,d</sup> does not seem necessary. While several attempts have been made<sup>6,9</sup> to connect the protein secondary structure (e.g.,  $\alpha$ -helix or  $\beta$ -sheet) with the surrounding water dynamics, our results suggest that no strong correlation should be expected, since the relevant topological parameter is more local and since an additional HB interaction strength should also be considered. However, while the dynamics is controlled by local factors, the impact of each residue cannot be straightforwardly transposed from the hydration dynamics of dilute amino acids. As shown in Figure 4a, the protein  $\rho_V$  and  $\rho_{HB}$  values are more widely spread than the values of dilute amino acids. This arises from the greater variety of local environments and especially topologies found in proteins: while a single amino acid is a simple convex solute, a protein surface exhibits a variety of pockets, clefts, and protrusions.

The dynamics investigated here pertains to the motion of individual water molecules. Beyond the simulation results, which, although in excellent agreement with NMR, may be slightly force-field dependent, we have identified parameter-free physical arguments which clearly indicate that most of the protein hydration layer is not dramatically retarded. Our results thus suggest that the very slow relaxations measured by techniques probing collective processes do not arise from very slow bound waters but rather from coupled protein–water motions,<sup>3k,15</sup> as also suggested for DNA hydration.<sup>16</sup> The same hydration slowdown factors identified here can be used to understand how hydration dynamics is affected in other biochemically relevant situations, including next to unfolded or misfolded proteins, at higher or lower temperatures, and in macromolecular assemblies. While the protein composition is anticipated to have a limited influence on the average water reorientation dynamics, our model should also be a valuable guide for the design of proteins with tailored local hydration dynamics leading to, e.g., enhanced catalytic activity, and contribute to the understanding of interfacial water dynamics in a wide range of biochemical assemblies.

## ■ ASSOCIATED CONTENT

### 📄 Supporting Information

Methodological details, including the simulation procedure, calculation of the reorientation time distribution, and parameters of the EJM. This material is available free of charge via the Internet at <http://pubs.acs.org>.

## ■ AUTHOR INFORMATION

### Corresponding Author

fabio.sterpone@ibpc.fr; damien.laage@ens.fr

### Present Addresses

<sup>‡</sup>Laboratoire de Biochimie Théorique, UPR9080 CNRS, IBPC, Paris

<sup>¶</sup>Department of Chemistry, Columbia University

### Notes

The authors declare no competing financial interest.

## ■ ACKNOWLEDGMENTS

We thank Casey Hynes (ENS Paris and Univ. of Colorado) for suggestions and encouragement, HPC Caspur (Rome) for computational resources (grant STD09-366), and the Foundation P.-G. de Gennes for financial support (F.S.).

## ■ REFERENCES

- (1) Levy, Y.; Onuchic, J. *Annu. Rev. Biophys. Biomol. Struct.* **2006**, *35*, 389.
- (2) (a) Klibanov, A. M. *Nature* **2001**, *409*, 241. (b) Eppler, R. K.; Komor, R. S.; Huynh, J.; Dordick, J. S.; Reimer, J. A.; Clark, D. S. *Proc. Natl. Acad. Sci. U.S.A.* **2006**, *103*, 5706. (c) Garczarek, F.; Gerwert, K. *Nature* **2006**, *439*, 109. (d) Grossman, M.; Born, B.; Heyden, M.; Tworowski, D.; Fields, G. B.; Sagi, I.; Havenith, M. *Nat. Struct. Mol. Biol.* **2011**, *18*, 1102.
- (3) (a) Bryant, R. G. *Annu. Rev. Biophys. Biomol. Struct.* **1996**, *25*, 29. (b) Halle, B. *Philos. Trans. R. Soc. London B* **2004**, *359*, 1207. (c) Mattea, C.; Qvist, J.; Halle, B. *Biophys. J.* **2008**, *95*, 2951. (d) Oleinikova, A.; Sasisanker, P.; Weingärtner, H. *J. Phys. Chem. B* **2004**, *108*, 8467. (e) Qiu, W.; Kao, Y.-T.; Zhang, L.; Yang, Y.; Wang, L.; Stites, W. E.; Zhong, D.; Zewail, A. H. *Proc. Natl. Acad. Sci. U.S.A.* **2006**, *103*, 13979. (f) Perticaroli, S.; Comez, L.; Paolantoni, M.; Sassi, P.; Lupi, L.; Fioretto, D.; Paciaroni, A.; Morresi, A. *J. Phys. Chem. B* **2010**, *114*, 8262. (g) Fenimore, P. W.; Frauenfelder, H.; McMahon, B. H.; Young, R. D. *Proc. Natl. Acad. Sci. U.S.A.* **2004**, *101*, 14408. (h) Hunt, N. T.; Kattner, L.; Shanks, R. P.; Wynne, K. *J. Am. Chem. Soc.* **2007**, *129*, 3168. (i) Mazur, K.; Heisler, I. A.; Meech, S. R. *J. Phys. Chem. A* **2011**, in press, DOI: 10.1021/jp2074539. (j) Russo, D.; Hura, G.; Head-Gordon, T. *Biophys. J.* **2004**, *86*, 1852. (k) Li, T.; Hassanali, A. A.; Kao, Y. T.; Zhong, D.; Singer, S. J. *J. Am. Chem. Soc.* **2007**, *129*, 3376. (l) Wood, K.; Plazanet, M.; Gabel, F.; Kessler, B.; Oesterheld, D.; Tobias, D. J.; Zaccai, G.; Weik, M. *Proc. Natl. Acad. Sci. U.S.A.* **2007**, *104*, 18049.
- (4) (a) Pizzitutti, F.; Marchi, M.; Sterpone, F.; Rossky, P. J. *J. Phys. Chem. B* **2007**, *111*, 7584. (b) Makarov, V. A.; Andrews, B. K.; Smith, P. E.; Pettitt, B. M. *Biophys. J.* **2000**, *79*, 2966. (c) Abseher, R.; Schreiber, H.; Steinhäuser, O. *Proteins* **1996**, *25*, 366. (d) Bizzarri, A. R.; Cannistraro, S. *J. Phys. Chem. B* **2002**, *106*, 6617. (e) Cheng, Y. K.; Rossky, P. J. *Nature* **1998**, *392*, 696. (f) Tarek, M.; Tobias, D. J. *Phys. Rev. Lett.* **2002**, *88*, 138101. (g) Marchi, M.; Sterpone, F.; Ceccarelli, M. *J. Am. Chem. Soc.* **2002**, *124*, 6787.
- (5) (a) Laage, D.; Hynes, J. T. *A Science* **2006**, *311*, 832. (b) Laage, D.; Stirnemann, G.; Sterpone, F.; Rey, R.; Hynes, J. T. *Annu. Rev. Phys. Chem.* **2011**, *62*, 395.
- (6) Sinha, S. K.; Bandyopadhyay, J. *J. Chem. Phys.* **2011**, *134*, 115101.
- (7) See Supporting Information.
- (8) (a) Garcia, A. E.; Hummer, G. *Proteins* **2000**, *38*, 261. (b) Rocchi, C.; Bizzarri, A. R.; Cannistraro, S. *Phys. Rev. E* **1998**, *57*, 3315. (c) Henchman, R. H.; McCammon, J. A. *Protein Sci.* **2002**, *11*, 2080.
- (9) (a) Nucci, N. V.; Pometun, M. S.; Wand, A. J. *Nat. Struct. Mol. Biol.* **2011**, *18*, 245. (b) Nucci, N. V.; Pometun, M. S.; Wand, A. J. *J. Am. Chem. Soc.* **2011**, *133*, 12326.
- (10) Tian, J.; Garcia, A. E. *J. Chem. Phys.* **2011**, *134*, 225101.
- (11) Luise, A.; Falconi, M.; Desideri, A. *Proteins* **2000**, *39*, 56.
- (12) (a) Laage, D.; Stirnemann, G.; Hynes, J. T. *J. Phys. Chem. B* **2009**, *113*, 2428. (b) Sterpone, F.; Stirnemann, G.; Hynes, J. T.; Laage, D. *J. Phys. Chem. B* **2010**, *114*, 2083.
- (13) Ji, M.; Odelius, M.; Gaffney, K. J. *Science* **2010**, *328*, 1003.
- (14) Laage, D.; Hynes, J. T. *Proc. Natl. Acad. Sci. U.S.A.* **2007**, *104*, 11167.
- (15) Nilsson, L.; Halle, B. *Proc. Natl. Acad. Sci. U.S.A.* **2005**, *102*, 13867.
- (16) Furse, K. E.; Corcelli, S. A. *J. Phys. Chem. Lett.* **2010**, *1*, 1813.